Hindawi
Advances in Materials Science and Engineering
Volume 2020, Article ID 1292513, 13 pages
https://doi.org/10.1155/2020/1292513

Research Article

Experimental Study of Friction Resistance between Steel and Concrete in Prefabricated Composite Beam with High-Strength Frictional Bolt

Qi Guo,[1] Qing-wei Chen ,[2] Ying Xing ,[1,3] Ya-ning Xu,[1] and Yi Zhu[2]

[1]*College of Civil Engineering, Taiyuan University of Technology, Taiyuan 030024, China*
[2]*Economic & Technology Research Institute of State Grid Shandong Electric Power Company, Jinan 250021, China*
[3]*College of Civil Engineering, Hunan University, Changsha 410082, China*

Correspondence should be addressed to Ying Xing; xingying_jamie@163.com

Received 12 June 2019; Accepted 4 January 2020; Published 19 February 2020

Academic Editor: Hongchao Kou

Prefabrication of composites beam reduces the construction time and makes them easily to be assembled, deconstructed, and partially repaired. The use of high-strength frictional bolt shear connectors can greatly enhance the sustainability of infrastructure. However, researches about the concrete-steel friction behavior are very limited. To provide a contribution to this area, 21 tests were conducted to measure the friction coefficient and slip stiffness with different concrete strength, steel strength, and surface treatment of steel. An effective finite element model was developed to investigate the ultimate bearing capacity and load-slip characteristics of bolt shear connection. The accuracy of the proposed finite element model is validated by the tests in this paper. The results demonstrate a positive correlation between concrete strength and friction coefficient and better performance of shot-blasted steel. It is also proved that high-strength frictional bolt has a 30% lower bearing capacity but better strength reserve and antiuplifting than the headed stud.

1. Introduction

As a result of the benefits of combining the advantages of its components, steel-concrete composite beams have been widely used in the high-rise buildings, multifloor industrial buildings, and bridges, which brings good economic and social benefits. The composite action of steel and concrete is realized by shear connectors, such as headed stud, channel steel, bend-up bar, and perforated ribs [1–3]. Among the shear connectors, headed stud is the most widely used one because of its rapid welding speed.

On the other hand, prefabricated construction has become a research focus on the view of environmental protection, because they can be easily assembled, deconstructed, and partially repaired [4]. However, for the common composite beam with headed stud cast into the concrete slab, it is difficult to just replace a failed connector without concrete broken. As a result, the repeated casting of concrete slab leads to more work, longer repairing time, and more material waste. Accordingly, to employ high-strength frictional bolt (HSFB), shear connectors instead of headed stud may reach a better results, as they can be unbolted to deconstruct the building or to alter part of it [5–7].

For the high-strength frictional bolt shear connectors, the shear resistance is provided by the friction between steel and concrete without any bonding, so the friction coefficient of the interface plays a key role in the structural design. Despite this, studies of the friction coefficient between steel and concrete are quite limited, while most studies in the open literature concentrate on the casting bonding behavior of the interface. Berthet carried two groups of push-out tests to evaluate the adhesion resistance of the composite structure with different connection types [8]. 16 groups of specimens were tested by Su and Du to measure the shear bond strength and friction coefficient of steel-concrete interface [9].

In order to measure the important coefficient, a series of 21 specific split tests were conducted systematically in this research, considering the effect of concrete strength, steel strength, surface treatment of steel, and the polypropylene fiber (PP fiber) added in the concrete. Based on the tests, failure modes of specimens and cracks of concrete were observed, and friction coefficients of concrete-steel interface were obtained. Moreover, the behavior of HSFB in composite beam was discussed through the finite element analysis.

2. Split Tests Program

2.1. Test Specimens. The test specimens were designed specifically to reflect the friction state of steel-concrete composite beam connected by high stress bolt. The loading way, bolt size, and steel plate thickness of test were similar with those of the real project, while the only difference is the thickness of concrete slab. A real concrete slab with the thickness of 100 mm at one side of steel plate was separated into two slabs of 45 mm at both sides of steel plate, in order to make the specimen convenient for axial loading, and makes the experiment easy to be achieved, as shown in Figure 1.

A specimen consisted of a $340 \times 120 \times 10$ mm steel plate and two $200 \times 100 \times 45$ mm concrete slabs. The concrete slabs were connected to the steel plate by two M16 high stress bolts through well-placed bolt holes. 8.8 grade bolts were used in the test with the tensile strength of 800 MPa and yield ratio of 0.8. Details of M16 high stress frictional bolts are shown in Figure 2.

Drilling holes in the concrete slabs lead to microdamage, which may develop into local cracks under the tremendous bolt preload. As a result, all the bole holes in concrete must be formed during casting to avoid any postprocessing. Before casting, steel tubes with the diameter of 19 mm were inserted into the steel mould and were separated from concrete slabs within 2 days after casting. The steel tubes were tightly covered by thin heat-shrinkable film in order to reduce the interface bounding, as shown in Figure 3. In this way, steel tube can be removed easily and hole shape can be remained.

The fiction surface of both concrete and steel ought to be smooth, clear, and dry without flash and strain. As a result, concrete slabs were cast in the uptight position, so the friction surface was not casting surface, as shown in Figure 4. For each kind of the concrete, 3 standard cubes with the dimensions of $150 \times 150 \times 150$ mm were prepared at the time that specimens were cast. All the specimens were cured in standard curing condition for more than 28 days.

Considering the lower accuracy of casting, enlarged bolt holes were employed on the concrete slabs to ensure the installation of bolts. The bolt boles on concrete were 3 mm larger than bolt in diameter, while the ones on steel plate were only 1.5 mm larger. Correspondingly, larger and thicker washers were adopted to protect concrete slab from local crushing shown in Figure 5.

There were 4 controlled variables in the test program including the compressive strength of concrete, the yield strength of steel, the polypropylene fiber added in the concrete, and the surface treatment of steel, which were considered the most important and potential factors in the real project of civil engineering.

According to the controlled variables, 21 specimens were classified into 7 groups. For each group, 3 same samples were tested to obtain the average results and eliminate accidental error. The details of variables are summarized in Table 1.

2.2. Specimen Assembling. Pretension of the bolt is another important factor affecting the friction of concrete-steel interface except friction coefficient. The torque that applied to high-strength frictional bolt can be read from the wrench, and the pretension of bolt can be calculated by

$$T_c = kP_t d, \tag{1}$$

where T_c is the final torque of high-strength bolt, k is the torque coefficient determined by geometry of the thread, P_t is the pretension force of high-strength blot, and d is the nominal diameter of the bolt. For the high-strength frictional bolts in the tests, k was 0.15.

High-strength friction bolts were screwed in two steps to make sure the friction surfaces were closed and the bolt pretension was uniform. The two steps were initial screwing and final screwing. The torque of initial screwing was about 50% of final screwing. Furthermore, bolts and washers must not be turned with nuts during the final screwing; otherwise, the bolt had to be changed.

All the concrete slabs could not be reinforced in this study on account of their small thickness of 45 mm. In the first few tests, pretension force was once set as 80 kN for 8.8 grade M16 bolts according to the Chinese Standard for Design of Steel Structures (GB50017-2017) [10]. However, the C40 and C50 concrete near the hole were crushed by tightened bolts due to the lower compressive strength. It is well known that the friction coefficient is only related to the contact surface and has no relationship with the pretension force. As a result, the entire pretension load for each bolt in this study was reduced to about 40 kN to protect concrete, while the test results were not affected.

2.3. Test Setup and Loading Procedures. Monotonic loading was applied by a 100 kN electrohydraulic servo testing machine. The specimen was set on a base plate that can rotate as spherical hinge so as to collimate actuator and steel plate. Two concrete blocks were put under the concrete slabs, so the steel plate did not touch the base. The loading setup is shown in Figure 6. All the specimens were preloaded before a formal test to remove the gap between testing machine and specimen. The preload was about 20% of the estimated slip load. Load control with the rate of 0.5 kN/s was used for the formal monotonic test.

In design, slip between concrete slab and steel plate means the failure of the high-strength frictional bolt, so the loading ought to be continued until slip appeared. However, the slip could be sudden, tiny, and hard to observe, as the gap between bolt shank and wall of hole was limited. Taken these

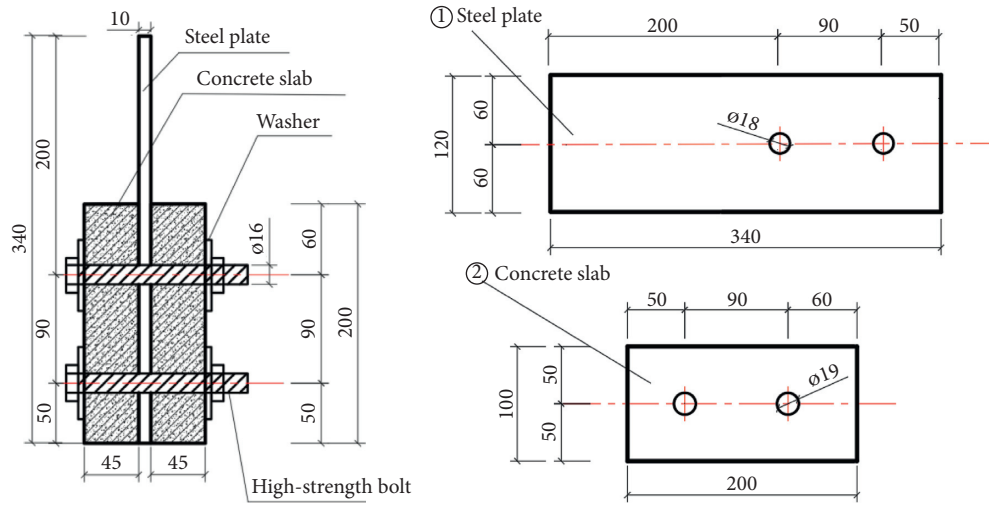

Figure 1: Details of specimen (mm).

Figure 2: M16 high-strength frictional bolt.

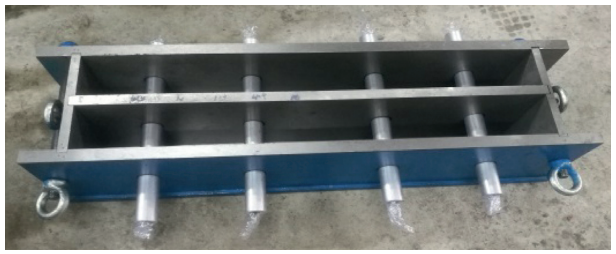

Figure 3: Steel mould and steel tubes.

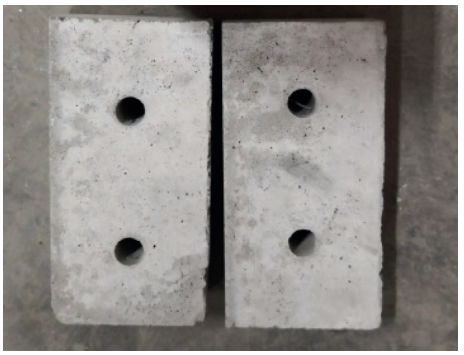

Figure 4: Concrete slabs with bolt hole.

Figure 5: Larger washers.

into consideration, the displacement jump in load-displacement curves was the only way to judge the slip moment. The load produced by the actuator and the displacement of the actuator were measured continuously throughout the entire test by the built-in transducer in the actuator, so as to show the load-displacement curves timely.

3. Test Results and Discussion

3.1. Slip-Load Curves and Failure Mode. Typical load-slip curves are shown in Figure 7. The whole process of test can be divided into 3 stages: friction stage, slip stage, and pressure stage. In Stage I, the shear load is entirely resisted by the static friction force, so the relative slip between steel and

Table 1: Summary of the test specimens.

Group	Specimen	Concrete	Steel	Surface treatment of steel
Group 1	S1–S3	C40	Q235	Shot-blasted
Group 2	S4–S6	C50		
Group 3	S7–S9	C60		
Group 4	S10–S12	C60 + PP fiber		
Group 5	S13–S15	C60	Q345	
Group 6	S16–S18	C60	Q235	Rusty
Group 7	S19–S21	C60	Q235	Cleaned by metal brush

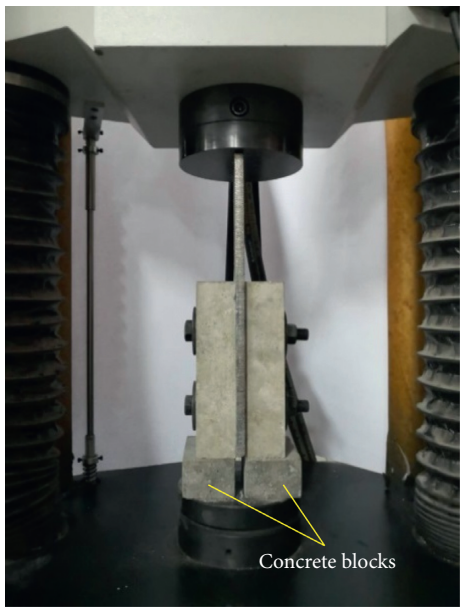

Figure 6: Loading setup.

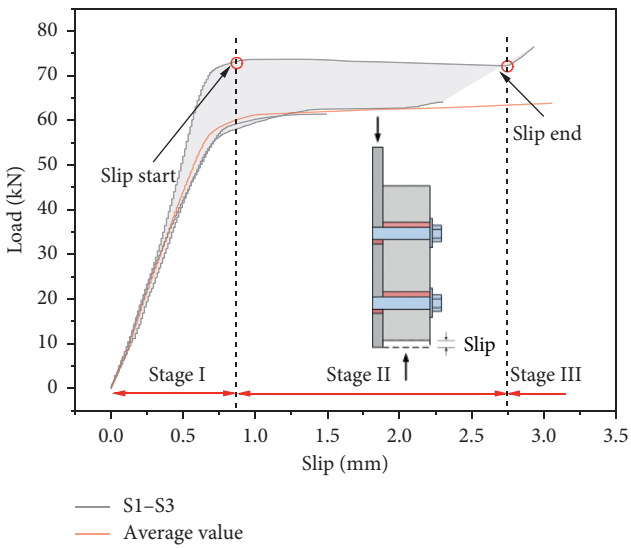

Figure 7: Load-slip curves.

concrete is quite small and the load-slip curves are basically linear.

When the load overcomes the maximum static friction force, the obvious slip begins to occur, and the test enters Stage II. The curves in this stage are almost horizontal, indicating that slipping occurred suddenly and developed rapidly. When the slip increases to a certain extent, the bolt shank contacts with the concrete hole wall; thus, the slip ends. The amount of slip occurred in Stage II depends on the space between the bolt shank and the bolt hole. Diameter of bolt was 16 mm, while the diameter of concrete hole was 19 mm. As a result, the ending slip is usually less than 3 mm in this stage.

Instead of friction between interfaces, mechanism of shear resistance in Stage III was changed into shear on bolt shank and pressure on the hole wall. In this way, the load can continue to increase. In this stage, the relative slip between steel plate and concrete slab is mainly caused by the deformation of bolts or the cracking of concrete slab, so the slip developed very slowly. If the test continued, the ultimate failure may be concrete hole crushing or bolt shank failure.

For high-strength frictional bolts, Stage I is the normal service state allowed in the design, while the bearing capacity provided in Stage II and Stage III is only used as strength reserve.

It can be seen from Figure 7 that the slip when static friction was overcoming is about 0.66~0.92 mm, and the stiffness of Stage I is about 88.3 kN/mm.

Two failure modes are possible in this steel-composite specimen: concrete cracking and slipping between concrete-steel interfaces. Failure mode of most specimens was simple: slip between concrete-steel interfaces without any other failure. For some other few specimens especially the ones used rusty and brush cleaned steel plate, slip occurred, while the concrete slab cracked. Effective sliding loads can be obtained in both failure modes above. However, only one specimen in Group 3 did not show significant slip, so the slip load could not be obtained, which may be caused by the hole diameter or installation error.

The result statistics show that concrete cracking occurred in only 2 of 15 specimens using shot-blasted steel plates, while concrete cracking occurred in 5 of 6 specimens using other surface treatments. Figure 8 shows the location of crack in concrete slab. All cracks began at the edge of the lower hole due to contact pressure between the bolt and the hole wall after slipping.

3.2. Slip Load and Friction Coefficient. The slip load and calculated friction coefficient of each specimen are summarized in Table 2. In the table, T_1 and T_2 are the final torque of two high-strength frictional bolts, respectively; $\sum P$ is the total pretension force of tow bolts; N_v is the load at the moment slip which occurs; μ is the friction coefficient; and $\overline{\mu}$ and s_μ are the mean value and standard deviation of the three same tests, respectively. The friction coefficient μ, as a function of load N_v, can be calculated by

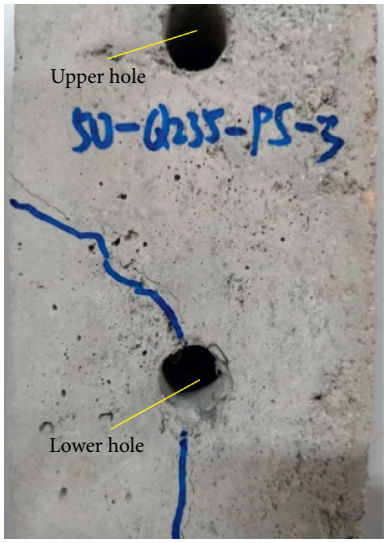

Figure 8: Cracks in concrete.

Table 2: Test results.

Group	Specimen	Final torque (N·m) T_1	T_2	$\sum P$ (kN)	N_v (kN)	μ	$\overline{\mu}$
Group 1	S1	100	100	83.3	59.5	0.357	0.377
	S2	102	102	85.0	73.2	0.431	
	S3	102	102	85.0	58.4	0.344	
Group 2	S4	100	98	82.5	61.6	0.373	0.390
	S5	100	100	83.3	65.2	0.391	
	S6	102	100	84.2	68.2	0.405	
Group 3	S7	—	—	—	—	—	0.444
	S8	100	100	83.3	74.1	0.445	
	S9	100	100	83.3	73.9	0.443	
Group 4	S10	100	104	85.0	64.4	0.379	0.420
	S11	102	102	85.0	69.7	0.410	
	S12	98	98	81.7	76.8	0.470	
Group 5	S13	102	102	85.0	70.8	0.416	0.458
	S14	100	100	83.3	85.6	0.514	
	S15	102	102	85.0	75.6	0.445	
Group 6	S16	100	100	83.3	54.0	0.324	0.358
	S17	102	100	84.2	60.0	0.356	
	S18	102	100	84.2	64.1	0.381	
Group 7	S19	100	100	83.3	53.8	0.323	0.285
	S20	100	100	83.3	49.3	0.296	
	S21	102	100	84.2	39.3	0.237	

$$\mu = \frac{N_v}{2\sum P}. \tag{2}$$

3.2.1. Concrete Compressive Strength. The only difference of specimens in Group 1~Group 3 is the compressive strength of concrete. It can be observed from Figure 9 that, with the increase of concrete strength, $\overline{\mu}$ shows an upward trend, especially for C60 concrete, whose friction coefficient is 12% higher than that of C50 concrete. Diversely, standard deviation s_μ decreased obviously with the increase of concrete strength, which means smaller dispersion and better reliability of higher strength concrete.

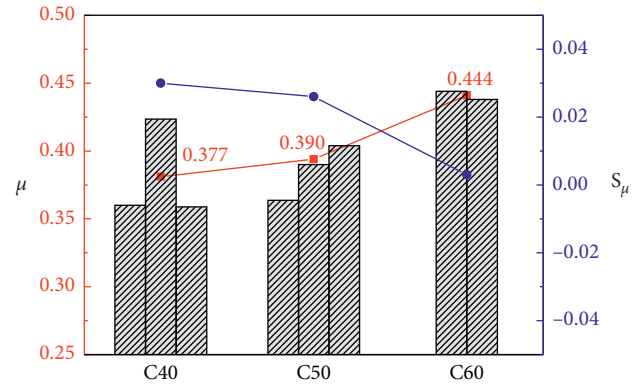

Figure 9: Effect of concrete strength on μ.

Different from the steel-steel surface, in the steel-concrete composite members, the factors affecting the friction coefficient test results are not only the roughness, but also two other factors: one is the surface hardness and the other is the crack resistance of concrete.

On the one hand, in the same degree of roughness, the greater the surface hardness, the higher the friction coefficient. The surface hardness of concrete is much less than that of steel, so the friction coefficient of the steel-concrete interface is controlled by the concrete which is easy to be damaged. In fact, the surface hardness of concrete has nothing to do with aggregate, but only with mortar. With a lower water-cement ratio in C60 concrete, the strength and hardness of mortar will be improved, which can effectively improve the friction coefficient.

On the other hand, under the pretension force of bolts, microcracks are more likely to appear in low-strength concrete, which lead to a small loss of actual bolt pretension, and the slip occurred at a lower load.

It can come to the conclusion that higher strength of concrete can improve the friction coefficient and reliability. Moreover, the pretension force of the bolt should be well matched with the strength of the concrete.

3.2.2. Polypropylene Fiber. Polypropylene fiber concrete is commonly used in the road and bridge deck due to its good ability of crack resistance. For the specimens made of C60 polypropylene fiber concrete and Q235 steel, friction coefficient of the interface was 0.420, which is about 5.4% smaller than the common C60 concrete, as shown in Figure 10 and Table 2.

There is macroscopic difference between the surface of common concrete and fiber added concrete, as shown in Figure 11. As polypropylene fibers are softer, some of them were exposed out of the concrete shortly, which lead to a gap between concrete and steel and prevent them from sticking together. Therefore, fibers have a negative effect on friction, but the effect is limited as the fibers are tiny.

3.2.3. Steel Strength. By comparing the results of Group 3 and Group 5, it can be seen from Figure 12 that the friction coefficient of the specimens using Q345 steel plate is only

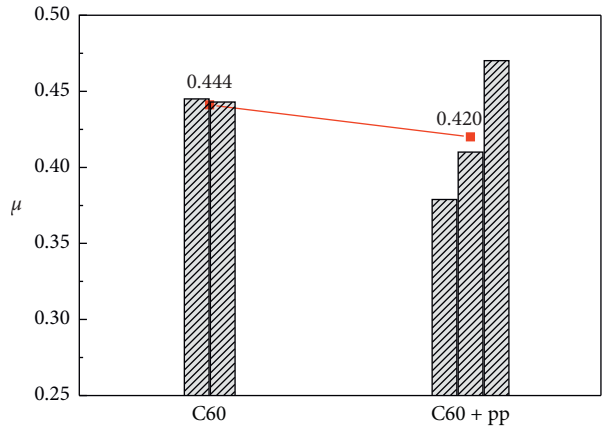

Figure 10: Effect of polypropylene fiber on μ.

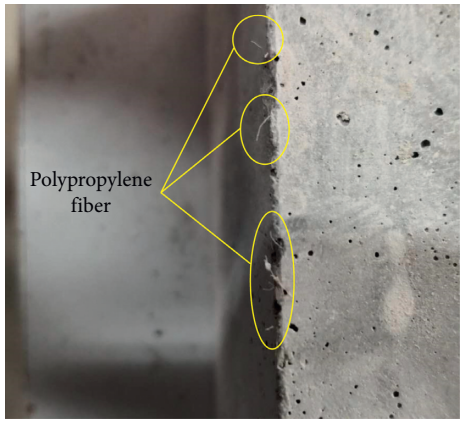

Figure 11: Polypropylene fiber on concrete surface.

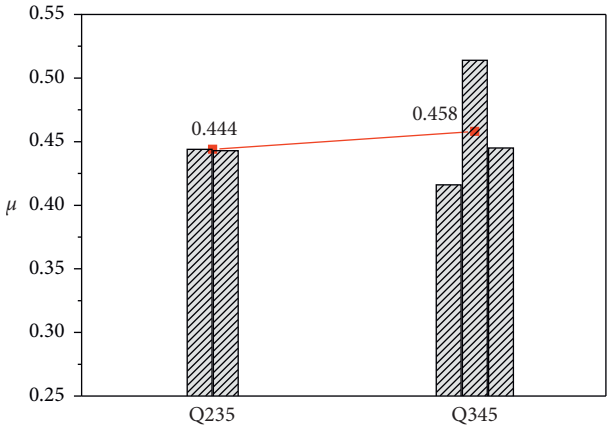

Figure 12: Effect of steel strength on μ.

3.2% bigger than that of Q235 steel plate, and the small difference can be attribute to the dispersion of the tests. This tendency shown in Table 3 is almost the same as the design value of steel-steel surface friction coefficient μ provided in the Chinese Standard [10].

3.2.4. Surface Treatment of Steel. Three different surface treatments used in Group 3, Group 6, and Group 7 were shot-blasted steel, rusty steel, and cleaned steel by metal brush, respectively. Figure 13 demonstrates the three kinds of surface appearances. As can be seen from Figure 14, compared with shot-blasted steel, the friction coefficient of rusty steel is reduced by about 19.4%, and that of cleaned steel is reduced by about 35.8%. This result is also correlated with the surface damage of concrete slab shown in Figure 15. Obvious metal scratches were evenly distributed on the concrete slab contact with shot-blasted steel, while the scratches became less and shallower on the concrete contact with loose rusty steel and cleaned steel.

This means that friction at the steel and concrete interface is caused by the intercalation and occlusion of surface protrusions.

Table 3: Comparison of μ with different steel.

Contact surface	Q235	Q345
Steel-steel surface	0.4	0.4
Steel-C60 concrete surface	0.444	0.458

4. Finite Element Simulation and Parametric Analysis

4.1. Geometry, Boundary Conditions, and Loading. A numerical analysis was conducted based on the test to further investigate the properties of the composite beam. In this analysis, the commercial finite element analysis software *ABAQUS* was used to simulate the test.

The solid element (C3D8R) was used for the concrete, steel beam, bolt, and washer members. Both geometric and material nonlinearity were considered in the finite element analysis. Fine hexahedral mesh was used for all the components to achieve accurate results.

Bottom surfaces of concrete slabs were constrained to the lower reference points, respectively, as shown in Figure 16. Reference points were then assigned with a fully fixed boundary condition.

Loading was defined in two subsequent steps corresponding to experimental testing: bolt preloading and loading up to failure. Bolts were preloaded by the "bolt load" method in *ABAQUS* to achieve the same pretension force of $P = 42$ kN as used in tests. Loading up to failure was applied as a vertical displacement $U_3 = 4$ mm of the upper reference point to which the top surface of the steel plate was constrained, as shown in Figure 16.

The interaction between the concrete slabs and steel plate is very important. General contact interaction procedure was used with normal behavior ("hard" formulation) and tangential behavior ("penalty" friction formulation). Friction coefficient obtained from the tests above was set for steel-concrete interface. Infinite friction stiffness is defaulted in the *ABAQUS* and there is no slip until friction is overcome. However, this assumption is obviously inconsistent with the experimental results, so the maximum elastic slip as 0.66~0.98 mm was another key parameter to be set in the simulation according to the tests results. No cohesion and same friction coefficient were used for the washer-concrete

(a) (b) (c)

Figure 13: Surface treatments of steel plate: (a) shot-blasted, (b) loose rusty, and (c) cleaned by metal brush.

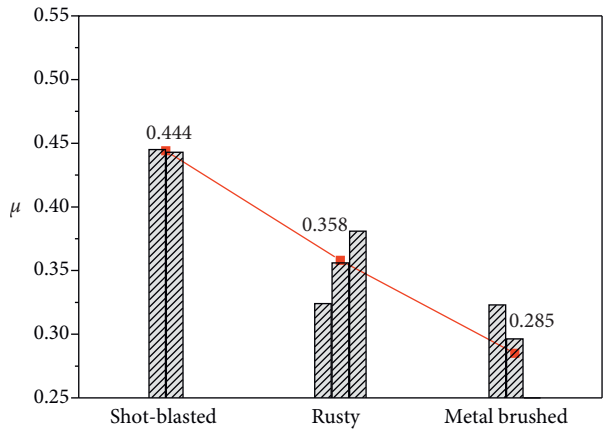

Figure 14: Effect of steel surface treatment on μ.

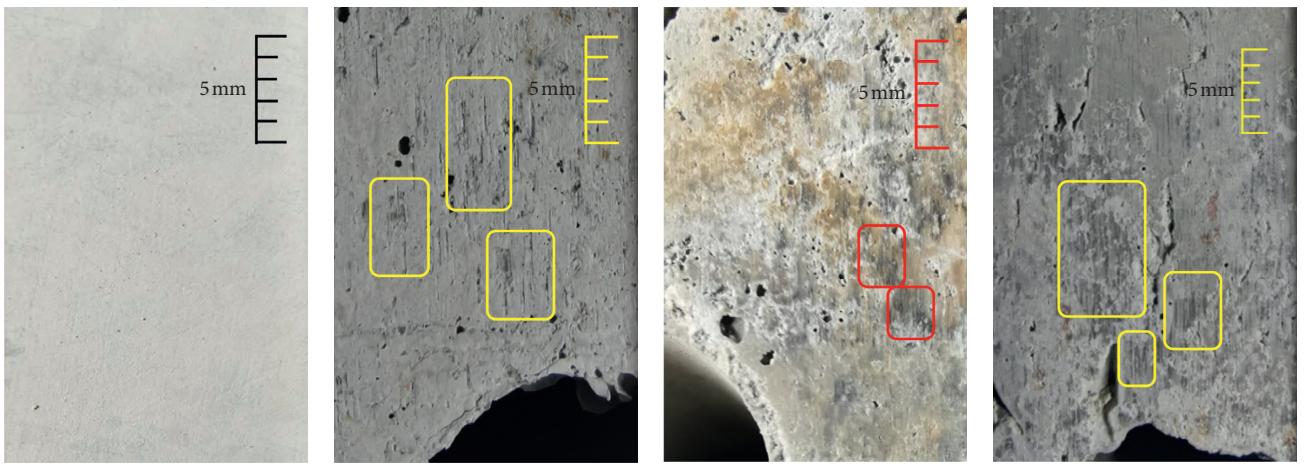

(a) (b) (c) (d)

Figure 15: Surface damage of concrete slab: (a) undamaged, (b) damaged by shot-blasted steel, (c) damaged by rusty steel, and (d) damaged by cleaned steel.

interface and washer-bolt head interface since it was greased during specimen preparation.

Moreover, with a "hard" formulation of normal behavior but "no friction" formulation of tangential behavior, general contact interaction procedure was applied between bolt and hole. In this way, the surfaces of bolt and hole were free to separate, but not to penetrate, which matched the real condition.

The concrete slab was the key members in the simulation; therefore, the elastic-plastic entire stress-strain curves were used in the simulation shown in Figure 17(a) [11]. As the pretension was only 42 kN for per bolt, the bolts

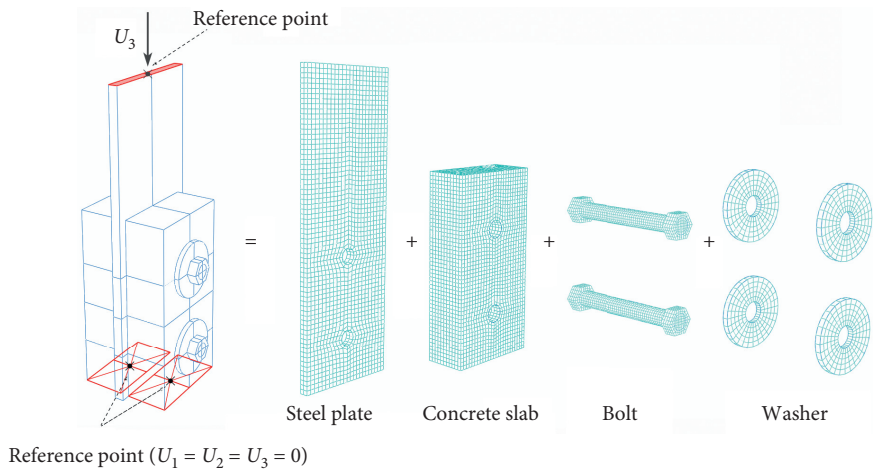

Figure 16: Boundary condition and loading surfaces of FEM model.

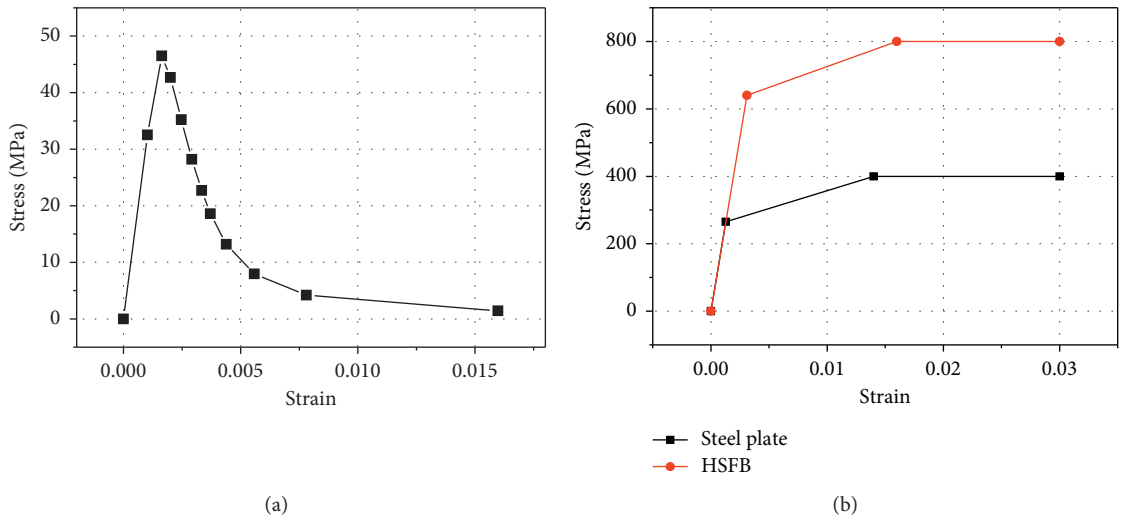

Figure 17: Stress-strain curves of the materials: (a) concrete and (b) steel plate and HSFB.

and steel plate were completely elastic in the tests. The simplified three-stage stress-strain curves were used for the bolt and steel plate member, as shown in Figure 17(b).

4.2. Validation of Simulation Result. Numerical load-slip curves of FEA models are compared with representative experimental load-slip curves in Figure 18. The main difference in the tests and FEA was the elastic stiffness; this can be attributed to the gap between the machine and the specimen and the discreteness of the small size specimen itself. For large scale structural components including many bolts, such as composite beams, the cooperation of multiple bolts will greatly reduce the discretization of single unite. It can be observed that the key values of the finite element analysis result exhibited a good agreement with the test data, including ultimate bearing capacity and elastic slip.

The deformation model of finite element analysis is also meeting the test phenomenon, as shown in Figure 19.

The deformation model of finite element analysis is also meeting the test phenomenon, as shown in Figure 19. Before the failure of friction, there was no contact between bolt and hole, corresponding to Stage I in the test; after friction failed, the steel plate hole contacted the bolt and derived it to move downward, corresponding to Stage II in the test; finally, bolt contacted the concrete hole and continued working, corresponding to Stage III. With the consideration of this, results of numerical analysis can be used for further analysis of failure modes and behavior of bolt shear connectors and headed stud.

4.3. Comparison of Bolt and Headed Stud Connector. Push-out test is a general standard test to study the shear capacity of shear connectors in composite beams. Full-size section like composite beams are usually used in the three components

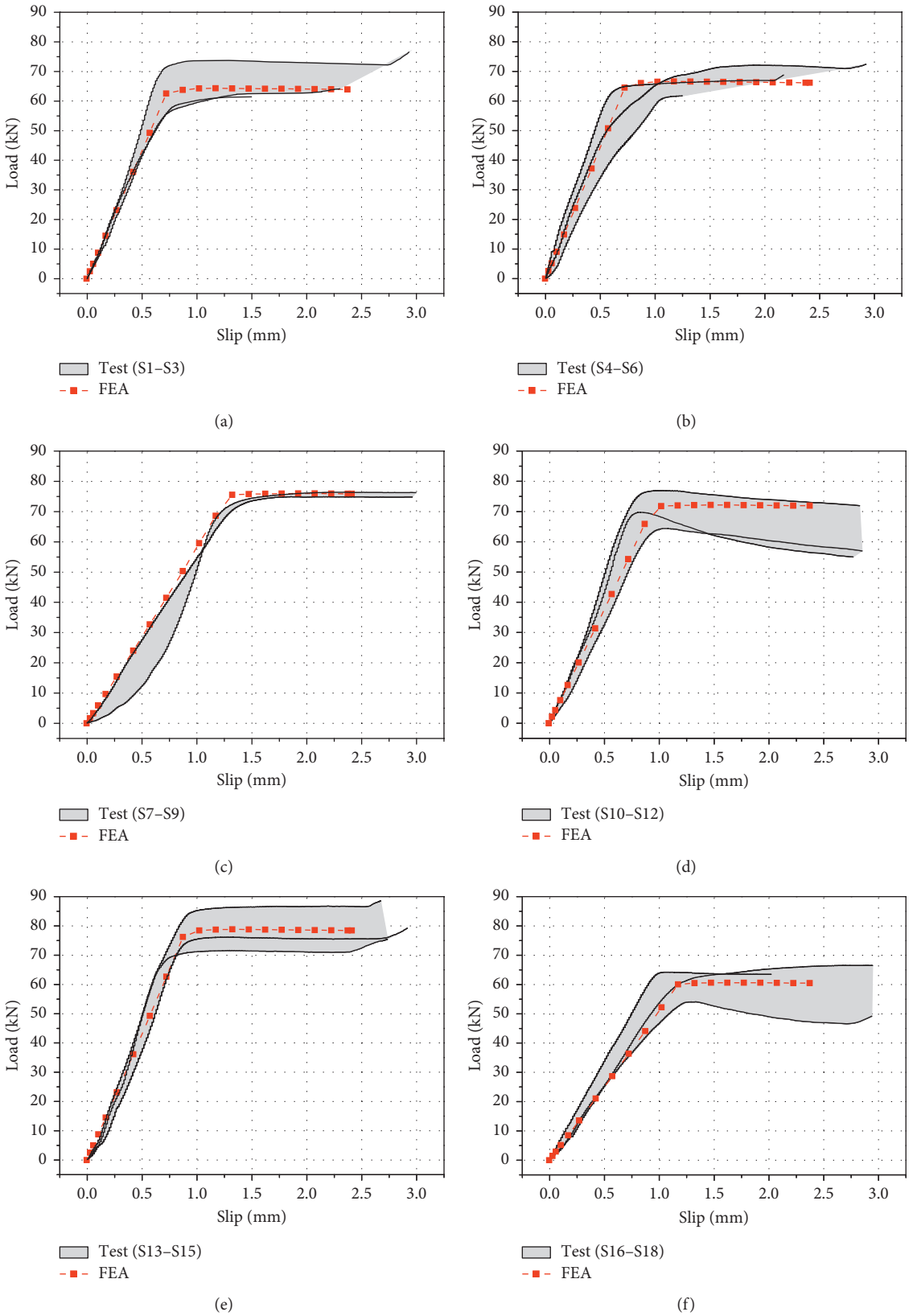

Figure 18: Continued.

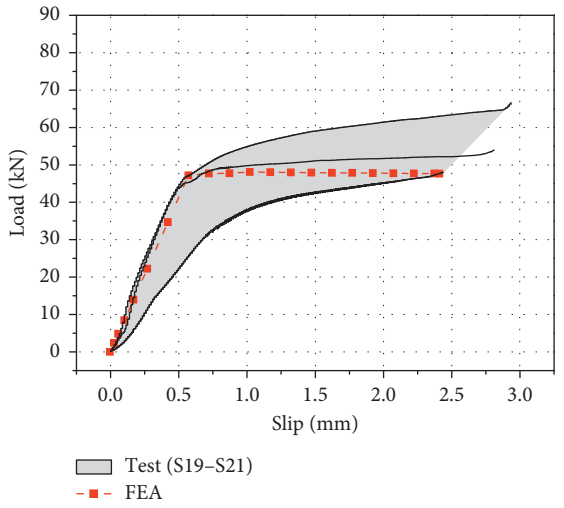

(g)

Figure 18: Comparison of load-slip curves: (a) Group 1, (b) Group 2, (c) Group 3, (d) Group 4, (e) Group 5, (f) Group 6, and (g) Group 7.

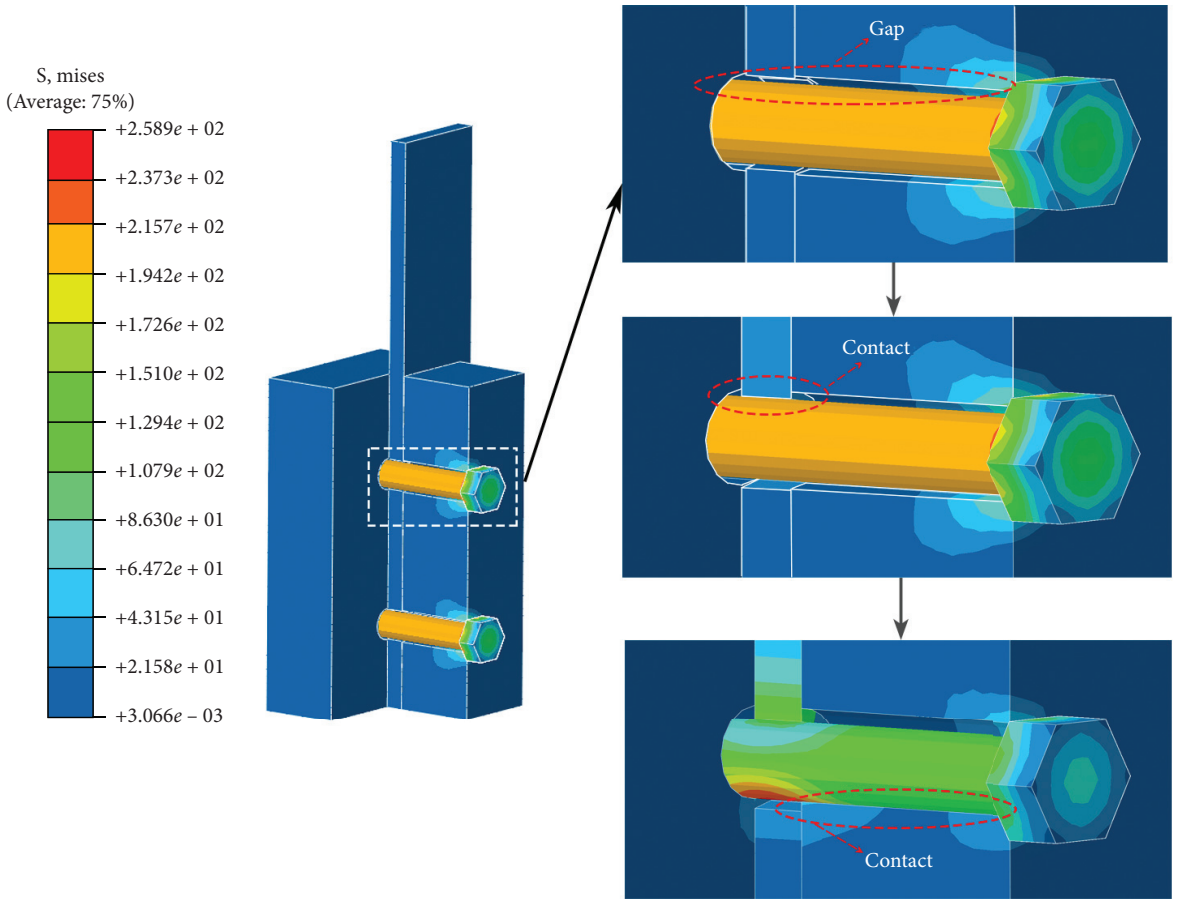

Figure 19: Deformation of finite element analysis.

of push-out specimen: H-shaped steel, concrete slabs, and shear connectors, in accordance with EC4 [12]. 18 push-out tests were undertaken to characterize the load-slip behavior of the different headed studs embedded in two kinds of concrete (Figure 20), among which 3 push-out tests used headed studs with diameter of 16 mm and common concrete [13].

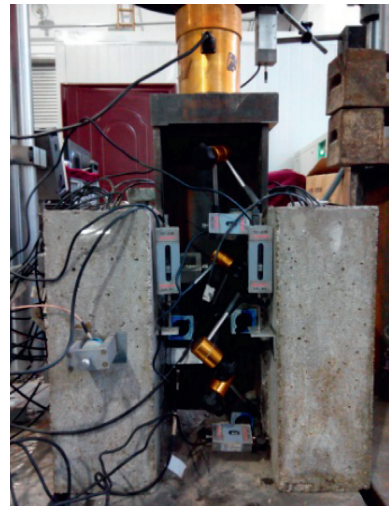

Figure 20: Push-out specimen with ϕ16 headed stud [13].

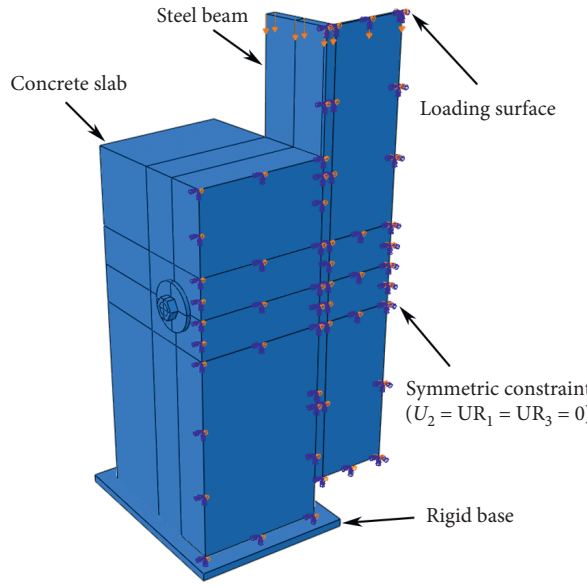

Figure 21: Push-out FEM with M16 HSFB.

In order to compare the behavior of frictional high-strength bolt and headed stud connector, the finite element model with the same size as the test in [13] was build, using M16 frictional high-strength bolt instead of 16 mm stud. Because of the symmetry of the specimens, only one-quarter of the push test arrangement was modeled, as shown in Figure 21. Corresponding symmetric constraints were applied, respectively, on the two symmetric surfaces. Discrete rigid body was set to model the ground. Furthermore, other details were set as the same way in validated FEM above including bolt hole dimension, interaction, mesh, load application, and material model. Better friction coefficient of Group 3 was adopted. Considering that the concrete plate of the specimen is reinforced, the pretension force of the high-strength bolt is filled up to 80 kN in accordance with its yield strength.

The load-slip curve obtained from the push-out tests are compared with that of bolted push-out simulation (see Figure 22). The curves indicate that the initial stiffness of two connectors was almost the same. Elastic and inelastic phases were obvious in the curve for headed stud. The proportional limit load P_p of headed stud was 45.5 kN, while the ultimate load P_u was 71.2 kN as design-bearing capacity. Specimen with HSFB is fully linear elastic within the usage phase before failure of friction, so its P_u of 32 kN is equal to P_p. As a result, the bearing capacity of high-strength frictional bolt is 30% lower than the headed stud in the same diameter. However, the reserve strength of bolt P_u' of 94.3 kN is much larger than the headed stud, because frictional bolt becomes into bearing type bolt after friction failed, and it can continue to work until shank or concrete hole failure.

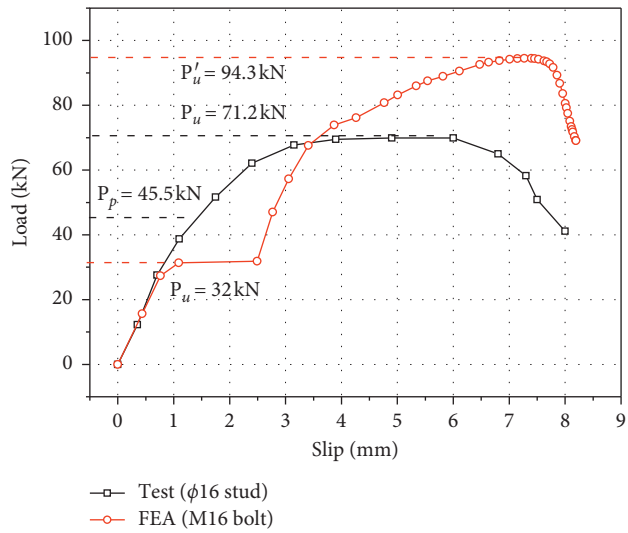

Figure 22: Load-slip curves of push-out test and FEA.

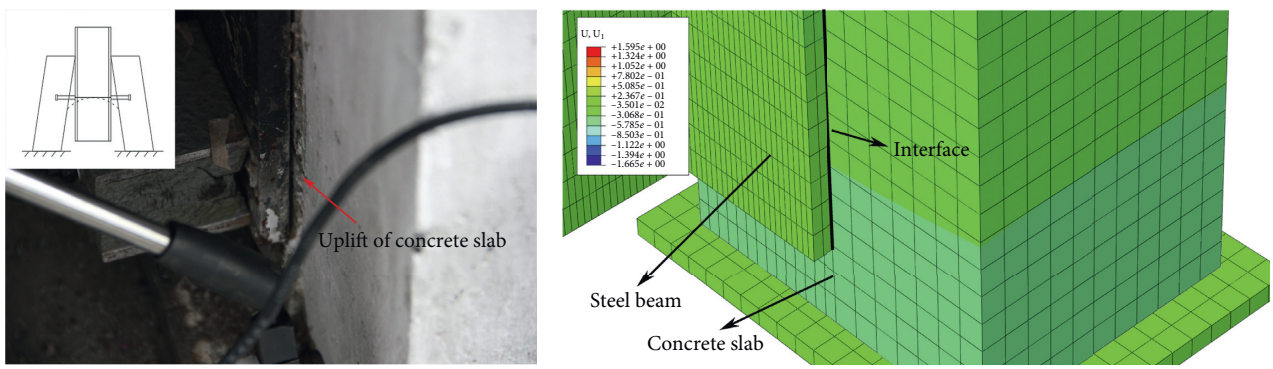

(a) (b)

Figure 23: Comparison of uplift of concrete slab: (a) concrete slab with headed stud [13] and (b) concrete slab with HSFB.

For the composite beam connected by headed stud, uplift of concrete slab was found as 1.7 mm in the test, which leads to a worse combination (see Figure 23(a)). In this way, the fully shear connected composite beam becomes into partial shear connected composite beam, and the bear capacity and stiffness would be decreased [14, 15]. Differently, for the composite beam connected by HSFB, the uplift of concrete slab was prevented effectively due to the pretension of HSFB (see Figure 23(b)).

5. Conclusions

This paper has described tests on specimens built up from a steel plate and two concrete slabs connected by high-strength frictional bolts. The motivation for the tests was to measure the friction coefficient of steel-concrete interface, which is an important basic parameter in the design of fabricated composite beams. 21 specimens were tested, and the response of each one was recorded. The influences of the concrete strength, steel strength, and surface treatment of steel were investigated.

Furthermore, a finite element model of push-out tests has been developed to investigate the behavior of high-strength frictional bolt shear connectors in composite beams using *ABAQUS* software. The results obtained from the experimental and simulative work have led to the following conclusions:

(1) It was found out that high-strength frictional bolts can be used as shear connectors in steel-concrete composite members, and the mechanical mechanism was the same as steel-steel members.

(2) By a series of tests, the friction coefficients of steel-concrete interface were obtained, which ranged from 0.377 to 0.458. The higher the concrete strength, the larger its friction coefficient. In addition, friction coefficients were affected by the surface treatment of steel, which is similar to that of steel-steel members. Shot-blasted steel is suggested in project.

(3) Pretension force was advised to be matched with a proper strength of concrete. As the compressive stress of concrete becomes larger, the reliability of

high-strength bolts connector decreased, and the use of high-strength bolts connector is inadvisable for strength concrete lower than C30.

(4) The use of high-strength frictional bolt as shear connectors in composite beams enables initial stiffness close to those with headed stud.

(5) Compared with conventional headed stud shear connectors, composite beams with high-strength frictional bolt have a lower ultimate bear capacity but higher strength reserve.

Data Availability

The data used to support the findings of this study are available from the corresponding author upon request.

Conflicts of Interest

The authors declare that they have no conflicts of interest.

Acknowledgments

The work in this paper was supported by the National Natural Science Foundation of China (no. 51708384), Natural Science Foundation of Shanxi Province, China (no. 201801D221216 and no. 201901D211017), and State Grid Science & Technology Project (no. SGSDJY00SJJS1900042).

References

[1] D. J. Oehlers and M. A. Bradford, *Composite Steel and Concrete Structural Members: Fundamental Behavior*, Pergamon, Oxford, UK, 1995.

[2] B. Jurkiewiez and J. M. Hottier, "Static behaviour of a steel-concrete composite beam with an innovative horizontal connection," *Journal of Constructional Steel Research*, vol. 61, no. 9, pp. 1286–1300, 2005.

[3] R. P. Johnson, *Composite Structures of Steel and Concrete: Beams, Slabs, Columns, and Frames for Buildings*, Blackwell Publishing, Oxford, UK, 2004.

[4] L. N. Dallam, *Push-out Tests with High Strength Bolt Shear Con- Nectors*, Department of Civil Engineering, University of Missouri-Columbia, Columbia, MO, USA, 1968.

[5] A. Ataei, M. A. Bradford, and X. Liu, "Experimental study of composite beams having a precast geopolymer concrete slab and deconstructable bolted shear connectors," *Engineering Structures*, vol. 114, pp. 1–13, 2016.

[6] G. Kwon, M. D. Engelhardt, and R. E. Klingner, "Behavior of post-installed shear connectors under static and fatigue loading," *Journal of Constructional Steel Research*, vol. 66, no. 4, pp. 532–541, 2010.

[7] G. Kwon, M. D. Engelhardt, and R. E. Klingner, "Experimental behavior of bridge beams retrofitted with postinstalled shear connectors," *Journal of Bridge Engineering*, vol. 16, no. 4, pp. 536–545, 2011.

[8] J. F. Berthet, I. Yurtdas, Y. Delmas, and A. Li, "Evaluation of the adhesion resistance between steel and concrete by push out test," *International Journal of Adhesion and Adhesives*, vol. 31, no. 2, pp. 75–83, 2011.

[9] Q.-T. Su, X. Du, C.-X. Li, and X. Jiang, "Tests of basic physical parameters of steel concrete interface," *Journal of Tongji University (Natural Science)*, vol. 44, no. 4, pp. 499–506, 2016, in Chinese.

[10] GB50017-2017, *Standard for Design of Steel Structures*, China Architecture and Building Press, Beijing, China, 2018, in Chinese.

[11] Y. Xing, Q. Han, J. Xu, Q. Guo, and Y. Wang, "Experimental and numerical study on static behavior of elastic concrete-steel composite beams," *Journal of Constructional Steel Research*, vol. 123, pp. 79–92, 2016.

[12] EN 1994-2, *Eurocode 4: Design of Composite Steel and Concrete Structures. Part 2: General Rules and Rules for Bridges*, BSI, Brussels, Belgium, 2004.

[13] Q. Han, Y. Wang, J. Xu, and Y. Xing, "Static behavior of stud shear connectors in elastic concrete-steel composite beams," *Journal of Constructional Steel Research*, vol. 113, pp. 115–126, 2015.

[14] S.-H. Kim, C.-Y. Jung, and J.-H. Ahn, "Ultimate strength of composite structure with different degrees of shear connection," *Steel & Composite Structures*, vol. 11, no. 5, pp. 375–390, 2011.

[15] J. Nie, J. Fan, and C. S. Cai, "Experimental study of partially shear-connected composite beams with profiled sheeting," *Engineering Structures*, vol. 30, no. 1, pp. 1–12, 2008.